Journal of Vibration and Acoustics. Received October 09, 2015;
Accepted manuscript posted March 6, 2017. doi:10.1115/1.4036110
Rolls-Royce plc

Novel frame model for mistuning analysis of bladed disc systems

Jie Yuan[1,4], Fabrizio Scarpa[1,3], Branislav Titurus[1,3], Giuliano Allegri[2], Sophoclis Patsias[5], Ramesh Rajasekaran[5]

[1]*Aerospace Engineering, University of Bristol, BS8 1TR Bristol, UK*

[2]*Department of Aeronautics, Imperial College London, London SW7 2AZ, UK*

[3]*Dynamics and Control Research Group, University of Bristol, BS8 1TR Bristol, UK*

[4]*Aerospace Division, Cranfield University, MK430AL, United Kingdom*

[5]*Rolls-Royce plc, PO Box 31, DE24 8BJ Derby, UK*

Corresponding author: Fabrizio Scarpa f.scarpa@bristol.ac.uk

Abstract

The work investigates the application of a novel frame model to reduce computational cost of the mistuning analysis of bladed disc systems. A full-scale finite element (FE) model of the bladed disc is considered as benchmark. The frame configuration for a single blade is identified through structural identification via an optimization process. The individual blades are then assembled by 3D springs, whose parameters are determined by means of a calibration process. The dynamics of the novel beam frame assembly is also compared to those obtained from three state-of-the-art FE-based reduced order models (ROMs), namely: a lumped parameter approach; a Timoshenko beam assembly; component mode synthesis (CMS) based techniques with free and fixed interfaces. The development of these classical ROMs to represent the bladed disc is also addressed in detail. A methodology to perform the mistuning analysis is then proposed and implemented. A comparison of the modal properties and forced response dynamics between the aforementioned ROMs and the full-scale FE model is presented. The case study considered in this paper demonstrates that the beam frame assembly can predict the variations of the blade amplitude factors and the results are in agreement with full-scale FE model. The CMS based ROMs underestimate the maximum amplitude factor, while the results obtained from beam frame assembly are generally conservative. The beam frame assembly is 4 times more computationally efficient than the CMS fixed-interface approach. This study proves that the beam frame assembly can efficiently predict the mistuning behavior of bladed discs when low order modes are of interest.

1. Introduction

A bladed disk typically consists in a set of disk-blade sectors that are designed to be identical. However, there are inevitable small variations in the structural properties of individual blades. These arise from manufacturing tolerances, statistical variations of material properties and/or geometric non-uniformity. The material and geometry uncertainties are further exacerbated by the operational wear and tear, as well as the non-conformal assembly of the blades [1]. These uncertainties will lead to the deviation of the blade natural frequencies (NFs) from their nominal design value; this phenomenon is commonly denoted as **mistuning**. The presence of mistuning can lead to mode localization, whereby the mechanical energy of the entire bladed disk can be transferred and confined to a subset comprising only few blades, or even a single blade [2, 3]. The maximum dynamic response of a mistuned bladed disc can be 5 times larger than the for a tuned one [4, 5]. The ensuing higher vibrational level is regarded as one of leading causes for shortened high cycle fatigue (HCF) life of mistuned discs. A significant amount of research effort has been devoted to address this problem since the 1960s'. One of the key aspects of mistuning analysis is how to quantify efficiently the effect of all the uncertainties mentioned above on the maximum dynamic response of bladed discs [6]. However, the mistuning problem is still considered a challenge from a design perspective, because of the high computational costs associated with the dynamic analysis, even when using state-of-the-art reduced order models (ROMs). The computational costs would be further increased when physical aspects like the non-linearity from the large geometry deformation of blades, contact friction in the dovetails and aerodynamic couplings are taken into account. The computational cost of mistuning prediction further increases if a reliability analysis is required. This is commonly based on probabilistic methods such as Monte Carlo simulations (MCS), which usually requires running thousands of simulation runs [7].

A basic bladed disk model is often represented by a cyclic chain of spring-mass oscillators with either one or two degrees of freedom (DOFs) for each sector [8]; this is a classical instance of a **lumped parameter model**. These models have been widely used at preliminary design stage, since they can capture some of the fundamental characteristics of bladed disc dynamics, despite their relative simplicity. The lumped parameter models have also proved suitable to investigate the statistics of the forced response in mistuned bladed disks. This requires the randomization of the lumped mass, damping and stiffness properties [9, 10]. However, the practical applicability of lumped parameters models is limited to the first three fundamental modes at most [9]. The Timoshenko beam model is commonly used in the aeroengine structural dynamics to represent the behavior of fan blades at the preliminary design stage. Beam models are very efficient from a computational point of view, but they are also able to capture the first few fundamental modes. The Timoshenko beam has however intrinsic limitations in terms of representing the coupling of bending and torsional modes for twisted fan blades [11]. The state-of-the-art ROMs for mistuning analysis are essentially based on using Finite Element (FE)-based modal reduction techniques, which can be broadly classified into two groups [9]. The first one includes techniques mainly developed between 1983 and 2000, and it mainly comprises component mode synthesis (CMS) methods [12-14]. CMS approaches assume that the blades and the disk are distinct sub-structural elements. Therefore their modes are separately calculated via deterministic FE analyses. The modal bases of the two substructures are then used to reduce the size of the overall system matrices, by enforcing compatibility conditions at the interfaces between the blade and the disk. The compatibility between the dynamic displacements existing within the interfaces of the substructures can be described by means of fixed-interface [15], free-interface [12] and hybrid-interface techniques [13]. The mistuning is then introduced into the blades in the form of natural frequency (NF) shifts. The choice of the interfacing method significantly affects the numerical convergence of the CMS-based ROMs. A fixed interface usually exhibit some very favorable convergence properties when increasing the number of component modes, but it also requires large numbers of interface DOFs and this penalizes the computational efficiency [16]. Another limitation of the fixed interface method is its inability to yield the constrained modes from testing, and this makes it suitable only for analytical or numerical models [17]. Free interface methods have slow convergence performance, although in principle this problem can be overcome by using residual flexibilities, i.e. attachment modes)[16]. These modes are usually obtained from low frequency approximations, hence the presence high frequency components is neglected [16]. Unfortunately, it is

difficult to extract accurate residual flexibility terms both from experimental data and analytical models [17]. The second group of ROMs is denoted System Mode based Models (SMM), which were pioneered by Yang and Griffin back in 2001 [18]. The main models belonging to this group include the Fundamental Mistuning Model (FMM) [8], the Component Mode Mistuning (CMM) [19] and the Integral Mode Mistuning [20]. The main concept behind the SMM is to employ selected sets of tuned system modes as a basis to represent the tuned disk-blade system, and then to project the mistuning effects into the system as perturbations. This strategy in principle allows an exact representation of the "baseline" tuned system. SMM techniques are also more computationally efficient than the CMS approaches. The first type of SMM algorithms includes Subset of Nominal Modes models (SNM) and FMM (please expand acronym of FMM) [8]. These models are based on the assumption that the modes of a mistuned bladed disk can be essentially represented by the linear combination of isolated blade modes of the tuned system, provided that the mistuning is small [21]. The accuracy of SMMs is very much dependent upon the modal representation of the tuned system. SMMs work well when the technique is applied to low order modes. However, for the analysis of the high order modes, practical industrial applications have shown that SMMs provide reliable predictive tools only if the extraction of hundreds of modes from FE full-scale models is carried out. SMM models are also unable to perform the mistuning analysis from the direct perturbation of specific parameters in the modal domain. Therefore, within the gas turbine industry, there is still a demand for simple mistuning analysis tools that can provide higher accuracy compared to lumped parameter models, but that also are less computationally expensive than CMS and SMM approaches.

In order to address some of the above issues, as a first step we have developed a novel ROM to represent the dynamics of a single blade [11]. Namely, we have introduced an equivalent beam frame model to describe the coupled flexural/torsional mode shapes, with their NFs and associated modal masses. The frame configurations are defined via a structural identification approach, based on a simulated annealing algorithm with stochastic tunneling. The approach is considerably more accurate than state-of-the-art blade ROMs based on traditional Timoshenko beams, and provides excellent accuracy with much reduced computational time when compared to high fidelity FE. The proposed model can adequately predict the global trends of the variations of the NFs when randomized lumped masses or material properties are used for mistuning analysis. As a further step from the previous work, the objective of this paper is to investigate the feasibility of using this novel beam frame assembly to increase computational efficiency for the mistuning analysis of a **whole** bladed disc. In this paper, all beam frames that represents the dynamics of the blades will be assembled using 3D springs to simulate the whole bladed disc dynamics, with the ensuing parameters determined through a calibration process (Figure 10). A full-scale FE model with 24 blades is considered as the reference model (Figure 1). We carry out a performance comparison of this novel ROM with respect to other state-of-the-art ROMs, namely a lumped parameter model (Figure 4), a Timoshenko beam assembly (Figure 6) and CMS-based ROMs (Figure 11). The development of the aforementioned three benchmark ROMs for representing the high fidelity dynamics are also described. A methodology to perform the mistuning analysis is then proposed and implemented. This is followed by the discussions of the modal properties and the forced response dynamics, comparing the ROMs to the full scale FE model.

2. Reference model

Figure 1 (a) shows the FE model of a bladed disc built by using the commercial software ANSYS Rel.15.0 (Ansys Inc, 2013). The rotor is entirely made of titanium, considered as a homogenous and isotropic material with Young's modulus of 115 GPa, density of 4800 kg/m^3 and Poisson's ratio of 0.32. Figure 1 (b) shows the zoomed view of a single blade, which has a high slenderness ratio (length to width: 10), and a uniform rectangular cross section. The model consists in 4,488 3D-SOLID (type 95) 20-node elements, with two elements spanning the thickness of both the blades and the disk. Each node has three translational DOFs; the total number of DOFs in the FE model is 80,064. The model is clamped at the inner circle of the disc by zeroing all DOFs. A convergence study of mesh size has been performed, demonstrating that the accuracy of the modal properties obtained from the FE model does not improve further by refining the mesh. A modal analysis has been then performed in ANSYS

using the Block Lanczos method. The simulations have been carried out on using a PC with an Intel 2.4GHz dual-core processor and 24 GB RAM. Considering the convergence criteria for the optimal performance of the Block Lanczos Method, 30% more modes are used. The convergence of this method is further validated by using 50% more modes.

Figure 2 shows the variations of the first five NFs against the nodal diameters (NDs) of the FE model that characterize the dynamical behaviors of a bladed disc. The fact that the disc itself becomes stiffer with increasing NDs makes the NFs of the rotor gradually increase, and finally approach the NFs of a single blade. The horizontal lines at high NDs represent the blade-dominated modes, while the lines with varying slope at low NDs represent disc-dominated vibrations. The nature of the blade-dominated modes at high NDs is indicated in the right column on the figure. However, the single blade mode may not be consistent throughout the ND range, because of the frequency "veering" phenomenon. The latter denotes the scenario when the NFs of two neighboring modes initially converge with the increase of NDs, but then veer apart without crossing [22]. Veering commonly occurs at low NDs. Modern bladed disks with low aspect ratio blades are particularly susceptible to frequency veering, because more vibration modes are usually packed into a relatively small frequency range, leading to increased chances of mode interaction. In this particular case study the frequency veering still occurs between the 4th and 5th modes, even though the blades have high aspect ratio (10) (see Figure 2). These two modes are coupled with each other for a ND number ranging from 6 to 9. With the further increase of NDs, the mode coupling disappears. In Figure 2 we can also observe a mode switch region, where the NFs of the first in-plane and second out-of-plane flapping mode intersect. In the veering and mode-intersection regions, there usually exist significant inter-blade couplings due to the high modal density [9]. This makes a mistuned bladed disc particularly sensitive to mode localization phenomena, as discussed in Section 1. The forced response of mistuned systems is therefore very sensitive to modes in the veering and intersection regions. This study is restricted to the analysis of the intersection region for low order modes.

Figure 3 shows the first six modes of the bladed disc sector of the full scale FE model. The spacing of the NFs in the first six modes are 1:3.66: 5.06:14.05:15.29:20.47 (note: NFs are normalized to the lowest natural frequency). The corresponding modes are first out-of-plane flap, first in-plane flap, second out-of-plane flap, third out-of-plane flap, first torsion and fourth out-of-plane flap, respectively. The out-of-plane modes dominate the dynamic behavior of the blade. The blade modes do not show significant coupling between bending and torsion. The modes listed above will be used as reference for the developments of the FE based ROMs in the following sections.

3. Lumped parameter model

Figure 4 shows the sketch of a 2 DOFs per sector lumped parameter model, with one DOF representing the motion of the blade and the other being related to the motion of the disk sector [10, 23, 24]. The bladed disc is described as a spring-mass multi-DOF system (1D). The blade DOF is associated with stiffness k^b and mass m^b; the parameters k^d and m^d represent the stiffness and mass of the disc. The stiffness k^c is related to the coupling between blades via the disc sector; q_i^b, q_i^d are the generalized coordinates of blade and disc in the i^{th} sector respectively. Engine order excitation is applied on the blade DOFs.

Formulation

The equation of motion (EoM) of the disc in i^{th} sector in presence of coupling from neighboring sectors is:

$$m^d \ddot{q_i^d} + \left(k^b + 2k^c + k^d\right) q_i^d - k^c\left(q_{i-1}^d + q_{i+1}^d\right) - k^b q_i^b = 0 \quad (1)$$

By taking the disc motion and external excitation into account, the EoM of the blade in i^{th} sector can be derived as:

$$m^b \ddot{q_i^b} + k^b\left(q_i^b - q_i^d\right) = f_i^b \tag{2}$$

From Eqs. (1) and (2), assuming harmonic oscillations in the whole system and the presence of structural damping, the equations of motions of the blade-disk system can be written in a matrix form as:

$$[-\omega^2 \boldsymbol{M} + (1 + \eta i)\boldsymbol{K}]\boldsymbol{q} = \boldsymbol{F} \tag{3}$$

In Eq. (3), η is the structural damping factor, $\boldsymbol{M}$, $\boldsymbol{K}$ are the global mass and stiffness matrices, while $\boldsymbol{q}$ and $\boldsymbol{F}$ represents the vectors of the dynamic displacements and external generalized forces, respectively. These matrices are expressed as:

$$\boldsymbol{M} = \begin{bmatrix} \boldsymbol{M^d} & \boldsymbol{0} \\ \boldsymbol{0} & \boldsymbol{M^b} \end{bmatrix},\ \boldsymbol{M^d} = m^d \boldsymbol{I}\,,\ \boldsymbol{M^b} = m^b \boldsymbol{I} \tag{4}$$

$$\boldsymbol{K} = \begin{bmatrix} \boldsymbol{K^d} & -\boldsymbol{K^b} \\ -\boldsymbol{K^b} & \boldsymbol{K^b} \end{bmatrix},\ \boldsymbol{K^b} = k^b \boldsymbol{I},\ \boldsymbol{K^d} = circ\,(\cdots, -k^c, k^b + 2k^c + k^d, -k^c, \cdots) \tag{5}$$

$$\boldsymbol{q} = \begin{bmatrix} \boldsymbol{q^d} \\ \boldsymbol{q^b} \end{bmatrix},\ \boldsymbol{q^d} = [q_1^d\,, q_2^d, \ldots, q_{N_b}^d]^{\,T},\ \boldsymbol{q^b} = [q_1^b\,, q_2^b, \ldots, q_{N_b}^b\,]^T \tag{6}$$

$$\boldsymbol{F} = \begin{bmatrix} \boldsymbol{f^d} \\ \boldsymbol{f^b} \end{bmatrix},\ \boldsymbol{f^d} = [0,0,\cdots,0]^T,\ \boldsymbol{f^b} = F_0[1, e^{j\phi_2}, \cdots, e^{j\phi_{N_b}}]^T,\ \phi_i = \frac{2\pi C(i-1)}{N_b} \tag{7}$$

In Eqs (4-7), $circ$ represents the circular repetition function (i.e. any given row is generated by a single column right shift of the row above). N_b represents the number of the blades, while C, ϕ_i are respectively the engine order number and phase angle of the excitation. The uncertainties in terms of the stiffness and mass properties of the bladed disc system are primarily due to the presence of the dovetail each blade and the disc, as well as the operational wear and tear at the loading edges and tips of the blades. These uncertainties significantly affect the actual blade stiffness, leading to the deviations of the nominal NFs with respect to design values. Therefore, the blade stiffness is randomized in this case study.

Parameter identification

The parameters of the lumped model are identified from the dynamics of the full-scale FE model shown in Figure 2, and, in particular, from the characteristic trends of the NF curves. It is worth noticing that this parametric identification cannot capture the specific mode shapes from the full-scale FE model, but it is used to identify the variation of the NFs at low NDs, i.e. within the intersection region highlighted in Figure 2. The calibration process adopted here follows the methodology proposed in [25] to identify the main lumped stiffness and mass parameters (k^b, k^c, k^d, m^d, m^b). The calibrated parameters of the lumped model are expressed in terms of non-dimensional stiffness and mass variables, as shown in Table 1. The dynamics of the lumped parameter and FE models will be discussed in Section 8.

4. Timoshenko beam assembly

Configuration identification of a single blade

Figure 5 shows the node locations of the Timoshenko beam elements in a sector of the full scale FE single blade model. The beam model consists of 9 3D Timoshenko beam elements, which are sufficient to approximate the first five modes of the blade. The first node, close to the radius of the disc, is fully clamped. The total number of the DOFs is 48. The cross-section properties of the elements are assumed to be the constant for the elements representing the blade part: these include area, bending and torsional inertias. The initial values of these properties are identified from the geometrical characteristics. For the first two elements that close to the radius, the "average" section properties are adopted accounting for the tapering of the dovetail. These beam properties are then tailored using an optimization procedure based on a Simulated Annealing algorithm in order to best represent the modal properties of the blade. The cost function used for the optimization includes NF errors and Modal Assurance Criterion (MAC) for the first five modes. The details of the implementation are similar to the optimization procedure used for beam frame configuration, and they can be found in [11].

Table 2 shows the comparison of the modal properties between the optimized Timoshenko beam model and the full scale FE model. For an untwisted blade, as that considered in this case study, the Timoshenko beam model is only able to represent the first four modes correctly, with the NF errors of 6.31%, 0.25%, 15.84% and 16.87%, respectively. Even though the modes are not affected by significant bending/torsional coupling, the simplified beam model still cannot capture the higher modes observed in the full-scale FE model.

Configuration identification of the assembly

Figure 6 shows the assembly of Timoshenko beams with 3D springs to couple the blades at their roots. As discussed in Section 1 and 2, the modes in the intersection region are very sensitive to the behavior of the mistuned rotor dynamics. In the worst-case scenario, mode localization can result in some blades having much larger vibrational amplitude factors (3-5 times) than their counterparts in the tuned system. The parameters of the connected springs are therefore identified based on the geometrical characteristics of the NF intersection region at low NDs. However, it is impossible to represent the complete intersection regions of the full-scale FE model via simple spring connections. The current study is therefore focused on approximating only the intersection region related to modes 2 and 3 (see the highlight in Figure 2). Therefore, only the first 3 modes of the rotor will be considered. The calibration process follows the methodology proposed in [25] to identify the main stiffness parameters. The results will be presented in the Section 7.

5. Beam frame assembly

Configuration identification for a single blade

Figure 7 shows the configuration of a beam frame model, which is used to represent the equivalent dynamics of a single bladed disc sector. The beam frame is constructed by using 12 3D Timoshenko beam elements, with a total number of 10 nodes. The beam frame model therefore has the same size of DOFs as the Timoshenko beam model discussed in Section 4. Figure 7 also illustrates the nodal positions of the frame with respect to the high-fidelity FE model. The two nodes at the radius of the disc (node 1 and 10) are fully clamped. The geometrical and material properties of the frame are consistent with those in the high-fidelity FE model. The beam cross-sectional properties (including areas and bending/torsional inertias) are estimated via structural identification equations coupled within an optimization process. The optimization strategy is based on the simulated annealing with stochastic tunnelling. The details of this identification procedure are presented in [11].

Figure 8 shows the auto MAC [23] of the first six modes when considering all the DOFs in the frame model. The maximum inter-mode correlation occurs between the mode 4 and mode 6 with a MAC value of 0.4, while all others MAC are below 0.2. These MAC values indicate that the current node selection in the frame model is sufficient to represent the first five modes of the blade. Figure 9 shows the comparisons of the NFs and the MAC between the optimal frame configuration and the reference model. The NF errors of the first five modes are extremely small (the maximum error is 0.4%) compared to the Timoshenko beam approach in Section 4. The MAC values between the beam frame and the full-scale FE model indicate the level of fidelity provided by the beam frame to capture all the first five modes of the full-scale FE. Since the maximum MAC value of any two modes is 1, we define in this paper the MAC error as 1-MAC. The maximum MAC error between the frame ROM and the high-fidelity FE model is 7% for the 5th mode. The MAC error increases with the mode number, and this is reasonable because the limited number of DOFs in the model hinders the description of complicated mode shapes for the higher modes, which are instead captured by the high-fidelity FE simulations.

Configuration identification of the assembly

Figure 10 illustrates the configuration of the frame awhen the blades are connected through 3D springs (kx, ky, kz). These represent the couplings between blades that take place through the disc. Similar to the identification method used for the Timoshenko beam ROM, the parameters of these springs are also determined based on the NF trends of the first three fundamental modes in the intersection region. This calibration process follows the methodology outlined in [25] to identify the main stiffness parameters. The modal properties obtained from this model are presented in the Section 7.

6. CMS-based ROM

Modal-based ROM techniques have been extensively used in the dynamic analysis of large structures. CMS based ROMs are here employed. Sub-structuring via a dedicated CMS module is available in the commercial FE software ANSYS 15. For the formulations of CMS methods with two different interfacing techniques, the reader is referred to [16]. A parametric study is carried out to investigate the convergence of these ROM techniques to find out the best performing boundary conditions of the CMS approach. This study involves varying the number of modes, the number of master DOFs, the interface method and the overall assembly strategy.

Two sub-structuring strategies

Figure 11 illustrates the two sub-structuring strategies that are considered in this case study. Figure 11 (a) shows the "blades with the disc assembly" (BDA) approach, whereby all the blades and disc are considered as individual components. The nodes on the interface between the blades and disc are used as master DOFs. Figure 11 (b) shows the "bladed-disc sector assembly" (BSA) approach, whereby the bladed disc is divided into 24 individual sectors.

Figure 12 shows the comparison of the relative NF errors from these two sub-structuring strategies discussed above with the same modal bases when comparing to the results from the full-scale FE model. This suggests that the use of the BSA approach is not sufficiently stable to represent the dynamics of the bladed disc, especially in terms of the out-of-plane flapping modes. The maximum NF errors of the first four out-of-plane flapping modes when using the BSA approach are respectively 2, 3, 6 and 4 times higher than their counterparts obtained using the BDA approach. One can also observe that the relative NF errors at low NDs are much larger than at high NDs when using the BSA

approach. This fact indicates that the BSA approach misrepresents the strong coupling between blades at low NDs due to the larger areas of the interface between the sectors. The forced response dynamics is however particularly sensitive to the modal behavior in the intersection region at NDs low for a mistuned bladed disc. Therefore, the BDA approach is a more suitable and efficient approach for a mistuning analysis.

Number of modes, master nodes & interface methods

Figure 13 shows the comparison of the relative NF errors resulting from a BDA approach using different number of modes for the bases. A fixed interface method is used to synthesize the modal components. The number of master nodes remains the same for all the modal bases considered (15 master nodes for each interface between blades and the disc). This case study considers four types of modal bases, resulting from the combinations of different numbers of blades and disc modes. The results are similar for all the modes. The relative NF errors do not reduce noticeably with an expansion of the modal basis, regardless whether more blade modes or disc modes are considered. This fact indicates that the BDA coupled with fixed interface method converges when a minimal number of modes are considered.

Figure 14 shows the comparison of the relative NF errors resulting from the BDA approach when considering a different number of master DOFs on the interface. The relative NF errors of the first three modes are reduced significantly by increasing the number of the master nodes in the interface from 10 to 21. With a further increase of the number of the master nodes to 25, the NF errors for all the six modes do not show any significant reduction. It can be therefore concluded that the ROM with the fixed interface method converges when 21 master nodes are used for each interface between the blade and the disc (about 57% of all the nodes in the interface).

Figure 15 shows the comparison of the relative NF errors between the BDA ROMs using fixed interface and free interface method. The fixed interface method with minimum convergent modal basis is used as a benchmark; this implies using 144 blade modes, 24 disc modes and 504 master nodes. However, using the same modal basis, the NFs resulting from the free interface model diverge for mode four, five and six. The free interface method converges when 10 modes of each blade are included in its modal basis. The free interface approach is more sensitive to the number of modes than the fixed interface method. This phenomenon is mainly attributed to the presence of rigid body modes in the modal analysis of the individual components. The results confirm the free interface method has slower convergence than the fixed interface approach, i.e. the free interface method requires a larger modal basis than for the fixed interface approach.

Best performing boundary conditions

As a result of the parametric study, the best configuration of the CMS-based ROM is the one with the fixed interface. The blade with the disc assembly (BDA) approach outperforms the bladed disc sector assembly (BSA) in terms of mode representation at low nodal diameters. Therefore, the fixed interface method with the BDA approach is here used as a representative CMS based ROM to benchmark the results ROM frame model

7. Methodology of the mistuning analysis

A methodology based on the lumped mass approach for mistuning analysis is described in this section. It includes mode selection, perturbation strategy, sensitivity study, mistuning pattern generation and external excitation. This methodology has been implemented for both the high-fidelity FE model and all ROMs described above.

Step 1. Selection of the modes

Figure 2 shows the variations of NFs with the NDs. The NFs of first and second mode families remain almost the same across the ND ranges. These isolated modes are not associated with significant couplings between the blades through the disc. However, the NFs for the 3rd and 4th modes show large gradients at low NDs, indicating some significant couplings between the blades. It is well known that the dynamic behavior of mistuned bladed disc are very sensitive to modes in the intersecting/veering region [9]. Therefore, the rotor 3rd mode (2nd out-of-plane flapping mode) at the 2nd ND is considered for the mistuning analysis in this work. Figure 16 shows the modal displacement of the chosen mode for the mistuning analysis.

Step 2. Introduction of the uncertainties

Based on the industrial experience, the major source of uncertainties in a blade disc derives from the dovetails between the blades and disc and damage in the blades due to the operational wear and tear [9]. These uncertainties in material and geometry lead to the deviations in the nominal NF values of the blade modes, to which forced rotor dynamics is very sensitive [23]. The NF deviations are therefore commonly used as the perturbations in modal based ROMs to represent the actual response uncertainties. In this case study, the lumped mass approach is used to introduce the perturbations from the geometry, representing equivalent NF deviations from experimental measurements. Either positive or negative NF deviations can be represented by lumped masses, as the corresponding values can be negative in FE analysis. Figure 17 shows the position where an additional mass is lumped. This is attached at the tip corner of blade, which is a critical region of the blades, since it suffers from geometrical changes due to damage caused by the wearing and impact during operations. Also, lumping a mass at the location of the maximum modal displacements (for the third mode that we have chosen) can help to keep the mass size minimum while achieving the desired NF deviations.

Step 3. Determination of the equivalent lumped masses

The sensitivity study is carried out for a single bladed disc sector to determine the magnitude of the lumped masses to represent the prescribed NF deviations. Cyclic boundary conditions are imposed on the surfaces between the sectors in the single bladed disc sector. All the nodes located on the surface of the inner circle are fully clamped. The ratios of lumped masses to the sector mass used in the study are $\pm 0.25\%, \pm 0.5\%, \pm 0.75\%, \pm 1.0\%$, respectively. Figure 18 shows the NF deviations of the first three modes decrease linearly with the increase of the lumped mass. The NF deviations of the first two flapping modes have a similar slope with respect to the lumped mass located at the tip of the blade. However, the gradient of the NF deviations in the 3rd flap mode is half than for the first two modes. A 2% deviation of the natural frequency can be generated by lumping 1% of the total sector mass. The large decrease of the NF deviation is mainly due to the more uniform distribution of the strain energy in the 3rd out of plane flap.

Step 4. Generation of the mistuning pattern

Based on the industrial practice (the reference cannot be disclosed yet), a 2% NF deviation is considered as the maximum perturbation level for the third flapping mode. The mistuning pattern for all the blades of the assembly is generated according to a uniform random distribution withing the limit of a $\pm 2\%$ NF deviation. The corresponding masses for each blade can be identified based on the

sensitivity study from the Step 3. Figure 19 shows the examples of corresponding lumped mass distributions associated with four different mistuning patterns.

Step 5. Application of the dynamic loading and damping

The engine order excitation is regarded as the main load in the gas turbines. When subjected to the engine order excitation, all the blades in an assembly would experience the same amplitude, but with different phase angles. The load can be split into a real part and an imaginary part. Figure 20 shows an example of the excitation corresponding to the 3nd engine order. In this case study, the 2nd engine order excitation is applied in a frequency range of 300-500 Hz. A structural damping value of 0.5% is considered.

8. Results and discussions

Comparison of the modal properties

Figure 21 shows the comparison of the variations of the NFs of the rotor with the NDs of the four ROMs considered (lumped parameter model, Timoshenko beam assembly, frame assembly and CMS based ROM approach). The modal analysis has been performed for all the presented ROMs using a Block Lanczos method in a PC with an Intel 3.2 GHz dual-core processor and 4 GB RAM.

Figure 21 (a) provides the direct comparison of modal properties between the lumped parameter model and the full scale FE model. A non-dimensional frequency $\xi = \frac{\omega}{\omega_0}$ is introduced, for which ω_0 corresponds to the NF of the "blade alone" mode in the lumped parameter model, calculated with the values of the non-dimensional stiffness and mass parameters. The two models show a general good agreement, in particular (as expected) within the intersection region at low NDs. It can be therefore stated that the lumped parameter model is able to represent coupling between the blades. The model can be also used to develop the fundamental understanding of the mistuning mechanism. However, it is also obvious that this model lacks the ability to represent the accurate dynamics of the flapping modes due to the limited number of DOFs considered. Therefore, it will not be further compared with the other ROMs in terms of mistuning analysis.

Figure 21 (b) and (c) show the variations of NFs in different NDs for the Timoshenko beam and frame assemblies respectively. These two ROMs are able to capture in a broad manner the NF crossing phenomenon between the first in-plane mode and second out-of-plane mode. The frame assembly however shows an enhanced ability to capture the high order modes, such as the 5th torsional one. Both ROMs only partially predict the variations of the 3rd out-of-plane mode. This is due to the fact that these two ROM describe the blade/disc interface in a relatively coarse fashion. The situation becomes worse for the higher order modes as these tend to exchange strain energy in a much more complicated way. In order to better capture the variations of the high order modes, a more sophisticated way to assemble the blades is necessary.

Figure 21 (d) shows the variations of NFs with the ND obtained from the CMS based ROM. The CMS techniques are implemented by using a "blades with disc assembly" (BDA) strategy and a fixed interfaced approach. Compared with beam frame assembly, the ROM is not only able to capture the NF crossing at the NDs, but it can also represent the NF variations in the high order modes such as 3rd out-of-plane one.

Comparison of the forced response

The mistuning analysis has been performed on the full-scale FE model and the other three ROMs with the same mistuning pattern (shown in Figure 19 mistuning pattern 1). Figure 22 shows the comparison

Journal of Vibration and Acoustics. Received October 09, 2015;
Accepted manuscript posted March 6, 2017. doi:10.1115/1.4036110
Rolls-Royce plc

of the distribution of the maximum blade amplitude factors between the full-scale FE model and three ROMs. For the CMS approach, the convergent modal bases and interfaces based on the previous case study are used. Figure 22 indicates that both the fixed and free interface methods yield a similar distribution of blade amplitude factors. The beam frame assembly and the CMS based ROM can capture the variations of the blade amplitude factor from the full-scale FE model. However, the CMS approach underestimates the maximum amplitude factor by about 20% for the 3rd, 10th, 15th and 18th blade. This makes the CMS approach less attractive for a conservative design of bladed discs, because the coupling of the inter-blades becomes a major factor in the forced response of the mistuned bladed disc. The CMS approach however lost some accuracy in describing the couplings between blades and disc when using the fixed interface method. On the contrary, the estimates of the maximum amplitude factors from the beam frame assembly are conservative, being 10% to 20% higher than the ones provided by the full-scale FE model. The reason behind this behavior is that a significantly higher strain energy density distribution is predicted at blade level in the frame compared to the full-scale FE model for the same external excitation. The Timoshenko beam assembly is not able to follow closely the variations of the maximum amplitude factor, although it has the same computational cost as the beam frame assembly. The peak values of the amplitude factor tend to shift right towards the next blade mainly because the Timoshenko beam cannot take into account the effect of the bending/torsional coupling, since the lumped mass is not located on the beam axis. Compared to the CMS approach, the Timoshenko beam further underestimates the maximum amplitude factors by about 15%.

Figure 23 shows the comparison of the CPU time between the ROMs and the full-scale FE model for 500 Monte Carlo simulations (MCS) of the mistuning problem. The CMS approach requires a significantly lower computing time than the full scale FE model, 65% less with the fixed interface method and 35% less with the free interface method. This result further confirms that the fixed interface method converges faster than the free interface one [16]. With a further increase of the simulation times, the computational advantage of using the CMS approach would be more obvious, because some procedures associated with using CMS-based ROMs are only required once for all the MCS, including the modal analysis of the components, perturbation projection and convergence study. These procedures however are very computational demanding. In comparison, the computing time of using the frame assembly is 13 times lower than for the full scale FE model, and 4 times lower than the most efficient CMS approach. The Timoshenko beam assembly requires a similar computing time to frame assembly because the size of these two models is the same in terms of number of DOFs.

9. Conclusions

This work provided a comparative study to assess the computational efficiency of a novel frame assembly for the mistuning analysis of bladed disc systems. Three classical ROMs were used as a benchmark, including a lumped parameter model, a Timoshenko beam assembly and a CMS-based model. The lumped parameter model can be used to represent efficiently the inter-blade modal couplings via a parametric identification. It is however not suitable to describe accurately the dynamics of high order modes due to the limited number of DOFs involved and the specific dynamics of mistuned bladed discs. The Timoshenko beam and the frame assemblies are able to capture the variations of the natural frequencies for the first few fundamental modes. The frame assembly greatly outperforms the Timoshenko beam model when representing higher order modes. However, the two models suffer from the approximated representation of the inter-blades coupling, in particular the ones affecting higher order modes. The accuracy of the CMS-based ROM depends on the use of assembly strategy, the interface method adopted, the number of modes and master nodes. The bladed disc sector assembly does not appear to be an efficient approach to represent the inter-blade coupling. With large areas of interface, the method requires a significantly greater number of master nodes than the blades with the disc approach. The convergence of the CMS approach is more sensitive to the number of

master nodes than the size of modal basis. The fixed interface method converges when about 57% of its interface nodes are used as masters. In comparison, the free interface method demands a significantly higher number of modes for convergence, because of the existence of rigid body modes. Compared to the beam frame assembly, the CMS approach is not only able to represent efficiently the inter-blade coupling at low order modes but also the veering phenomena affecting the high order modes.

The work presented in this paper has also addressed the implementation of a methodology to perform the mistuning analysis of bladed discs, which is based on the lumped mass perturbation. The frame assembly can capture the variations of the blade amplitude factors in good agreement with the full-scale FE model. Unlike the CMS-based ROMs, the forced responses obtained from the frame assembly are more conservative. This feature can make the frame model more attractive as a design tool of bladed discs, since conservative solutions are always preferred at a preliminary design stage. A Timoshenko beam assembly with the same number of DOFs as the frame model does not predict accurately enough the variations of the maximum amplitude factor. The peak values of the amplitude factor tend to shift right to the next blade. One of the main reasons behind this behavior is that in a Timoshenko beam assembly is difficult to take into account the geometrical location of lumped masses accurately, especially if the masses are not placed on the symmetry axis. Compared to the CMS approach, the Timoshenko beam assembly further underestimates the peaks of maximum amplitude factor by about 15%. With respect to the computational costs, the CMS approach with fixed interface method requires 65% less CPU time than the full scale FE model, and 35% less with free interface method. As expected, the beam frame assembly requires 4 times less than the CMS approach with the fixed interface method. The computational costs associated with Timoshenko beam approach are similar to those of the frame assembly. The case study shows that the beam frame assembly is a viable tool for mistuning analysis of bladed discs when low order modes are of interest.

Acknowledgements

The authors would like to acknowledge the support of Rolls-Royce plc for the support of this research through the Composites University Technology Centre (UTC) at the University of Bristol, UK. Special acknowledgement goes also to the Strategic Investment in Low carbon Engine Technology (SILOET) programme supported by Rolls-Royce plc and Technology Strategy Board (TSB), and to the China Scholarship Council.

Reference

[1] Ewins, D., and Han, Z., 1984, "Resonant vibration levels of a mistuned bladed disk," Journal of Vibration Acoustics Stress and Reliability in Design, 106, p. 211.
[2] Chen, Y., and Shen, I., 2015, "Mathematical Insights Into Linear Mode Localization in Nearly Cyclic Symmetric Rotors With Mistune," Journal of Vibration and Acoustics, 137(4), p. 041007.
[3] Chandrashaker, A., Adhikari, S., and Friswell, M., 2016, "Quantification of vibration localization in periodic structures," Journal of Vibration and Acoustics, 138(2), p. 021002.
[4] MacBain, J., and Whaley, P., 1984, "Maximum resonant response of mistuned bladed disks," Journal of Vibration Acoustics Stress and Reliability in Design, 106, p. 218.
[5] Whitehead, D., 1998, "The maximum factor by which forced vibration of blades can increase due to mistuning," Journal of Engineering for Gas turbines and Power, 120(1), pp. 115-119.
[6] Han, Y., and Mignolet, M. P., 2015, "A Novel Perturbation-Based Approach for the Prediction of the Forced Response of Damped Mistuned Bladed Disks," Journal of Vibration and Acoustics, 137(4), p. 041008.
[7] Au, S.-K., and Beck, J. L., 2001, "Estimation of small failure probabilities in high dimensions by subset simulation," Probabilistic Engineering Mechanics, 16(4), pp. 263-277.

[8] Feiner, D. M., and Griffin, J., 2002, "A fundamental model of mistuning for a single family of modes," Journal of turbomachinery, 124(4), pp. 597-605.
[9] Castanier, M. P., and Pierre, C., 2006, "Modeling and Analysis of Mistuned Bladed Disk Vibration: Current Status and Emerging Directions," Journal of Propulsion and Power, 22(2), pp. 384-396.
[10] Lee, S.-Y., Castanier, M. P., and Pierre, C., "Assessment of probabilistic methods for mistuned bladed disk vibration," Proc. Proceedings of the 46th AIAA/ASME/ASCE/AHS/ASC Structures, Structural dynamics, and Materials Conference, AIAA-2005-1990.
[11] Yuan, J., Allegri, G., Scarpa, F., Rajasekaran, R., and Patsias, S., 2015, "Novel parametric reduced order model for aeroengine blade dynamics," Mechanical Systems and Signal Processing, 62, pp. 235-253.
[12] Irretier, H., 1983, "Spectral Analysis of Mistuned Bladed Disk Assemblies by Component Mode Synthesis," Vibrations of Bladed Disk Assemblies, D. J. E. A. V. Srinivasan, ed., American Society of Mechanical Engineers, New York.
[13] Óttarsson, G., 1994, "Dynamic modeling and vibration analysis of mistuned bladed disks," University of Michigan.
[14] Yang, M.-T., and Griffin, J., 1997, "A reduced order approach for the vibration of mistuned bladed disk assemblies," Journal of Engineering for Gas turbines and Power, 119(1), pp. 161-167.
[15] Joo, W., Yee, K., Lee, D.-H., and HURTY, W., 1965, "Dynamic analysis of structural systems using component modes," AIAA journal, 3(4), pp. 678-685.
[16] Petyt, M., 2010, Introduction to finite element vibration analysis, Cambridge university press.
[17] Butland, A., and Avitabile, P., 2010, "A reduced order, test verified component mode synthesis approach for system modeling applications," Mechanical Systems and Signal Processing, 24(4), pp. 904-921.
[18] Yang, M.-T., and Griffin, J., 2001, "A reduced-order model of mistuning using a subset of nominal system modes," Journal of Engineering for Gas turbines and Power, 123(4), pp. 893-900.
[19] Lim, S.-H., Bladh, R., Castanier, M. P., and Pierre, C., 2007, "Compact, Generalized Component Mode Mistuning Representation for Modeling Bladed Disk Vibration," AIAA Journal, 45(9), pp. 2285-2298.
[20] Vargiu, P., Firrone, C. M., Zucca, S., and Gola, M. M., 2011, "A reduced order model based on sector mistuning for the dynamic analysis of mistuned bladed disks," International Journal of Mechanical Sciences, 53(8), pp. 639-646.
[21] Yang, M.-T., and Griffin, J., 1997, "A normalized modal eigenvalue approach for resolving modal interaction," Journal of Engineering for Gas turbines and Power, 119(3), pp. 647-650.
[22] Kenyon, J., Griffin, J., and Kim, N., 2004, "Frequency veering effects on mistuned bladed disk forced response," Journal of propulsion and power, 20(5), pp. 863-870.
[23] Griffin, J., and Hoosac, T., 1984, "Model development and statistical investigation of turbine blade mistuning," Journal of Vibration Acoustics Stress and Reliability in Design, 106, p. 204.
[24] Yuan, J., Allegri, G., Scarpa, F., Patsias, S., and Rajasekaran, R., 2015, "numerical assessment of using Sherman-Morrison, Neumann expansion techniques for stochastic analysis of mistuned bladed disc systems," Proceedings of ASME Turbo Expo 2015: Turbine Technical Conference and Exposition, ASME, Montréal, Canada
[25] Baik, S., Castanier, M. P., and Pierre, C., "Mistuning sensitivity prediction of bladed disks using eigenvalue curve veerings," Proc. Proceedings of the 9th National Turbine Engine High Cycle Fatigue Conference.

Figure caption list

Table Heading list

Journal of Vibration and Acoustics. Received October 09, 2015;
Accepted manuscript posted March 6, 2017. doi:10.1115/1.4036110
Rolls-Royce plc

Figure list

(a) (b)

Figure 1 Finite element model of (a) a bladed disc and (b) a single blade sector

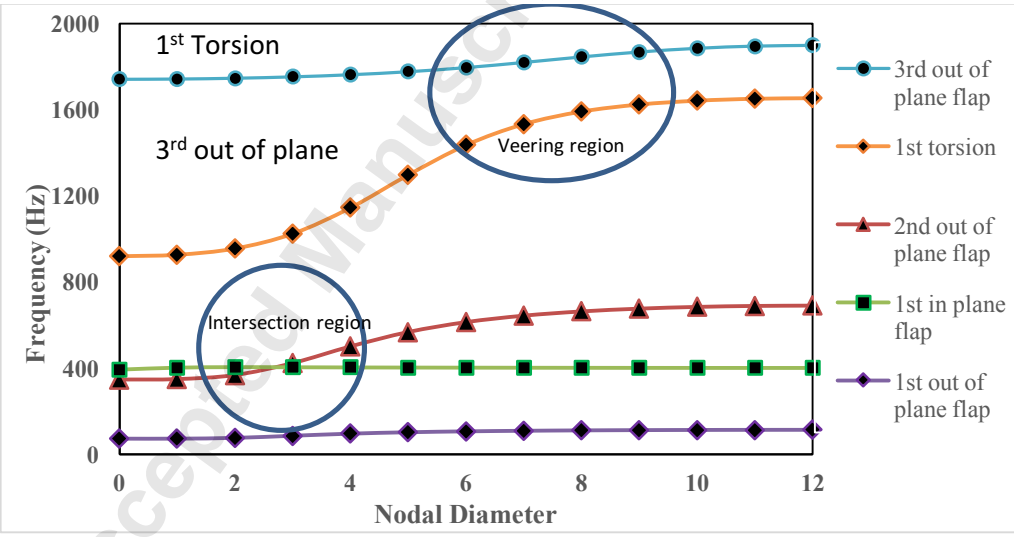

Figure 2 Natural frequencies versus nodal diameters (FE)

Journal of Vibration and Acoustics. Received October 09, 2015;
Accepted manuscript posted March 6, 2017. doi:10.1115/1.4036110
Rolls-Royce plc

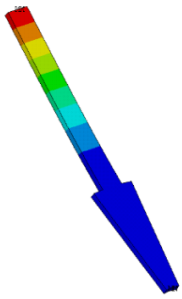

Mode 1 1st out of plane flap

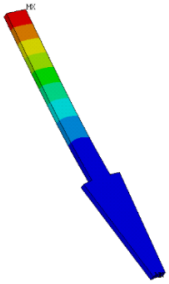

Mode 2 1st in plane flap

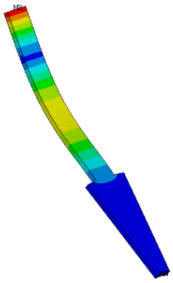

Mode 3 2nd out of plane flap

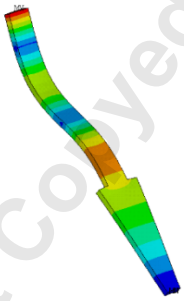

Mode 4 3rd out of plane flap

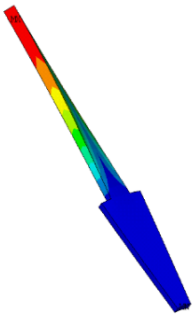

Mode 5 1st torsion

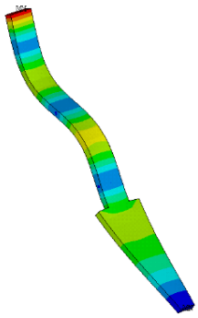

Mode 6 4th out of plane flap

Figure 3 Mode shapes of the first six modes of the sector

Journal of Vibration and Acoustics. Received October 09, 2015;
Accepted manuscript posted March 6, 2017. doi:10.1115/1.4036110
Rolls-Royce plc

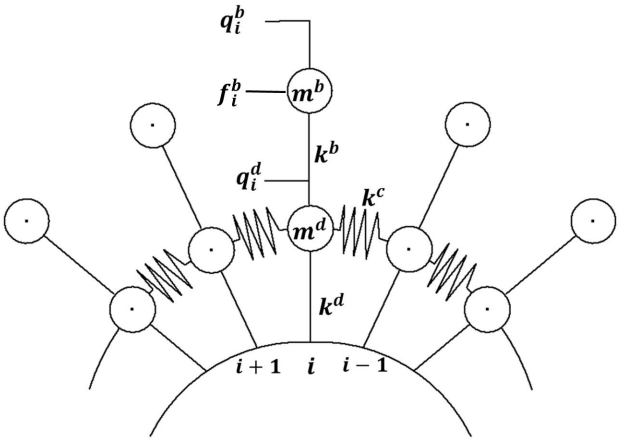

Figure 4 Two DOFs per sector mode

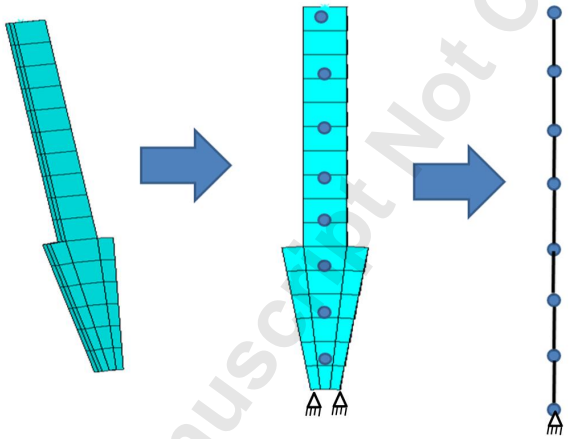

Figure 5 Timoshenko beam approximation based on the FE sector

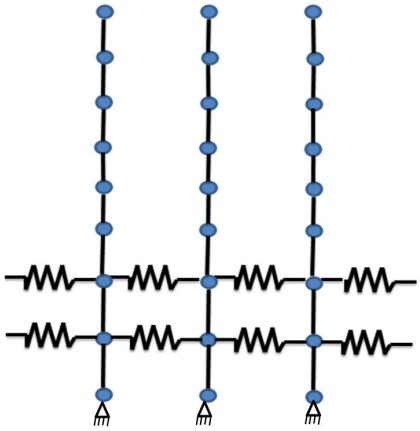

Figure 6 Assembly of the Timoshenko beams with the coupling springs

Journal of Vibration and Acoustics. Received October 09, 2015;
Accepted manuscript posted March 6, 2017. doi:10.1115/1.4036110
Rolls-Royce plc

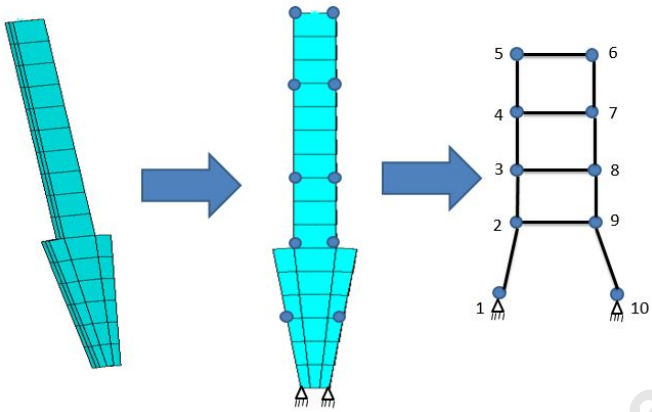

Figure 7 beam frame sector approximation based on FE sector

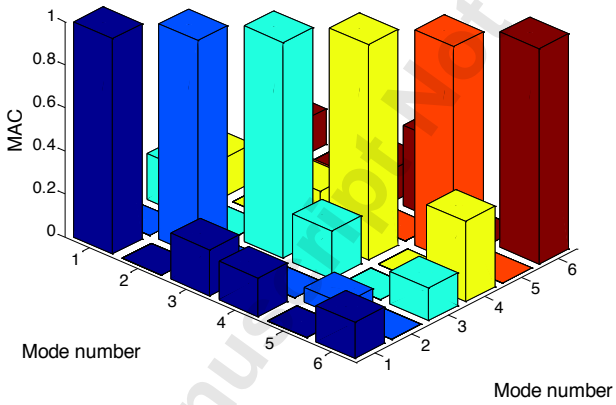

Figure 8 Auto MAC of the first six modes with 10 nodes

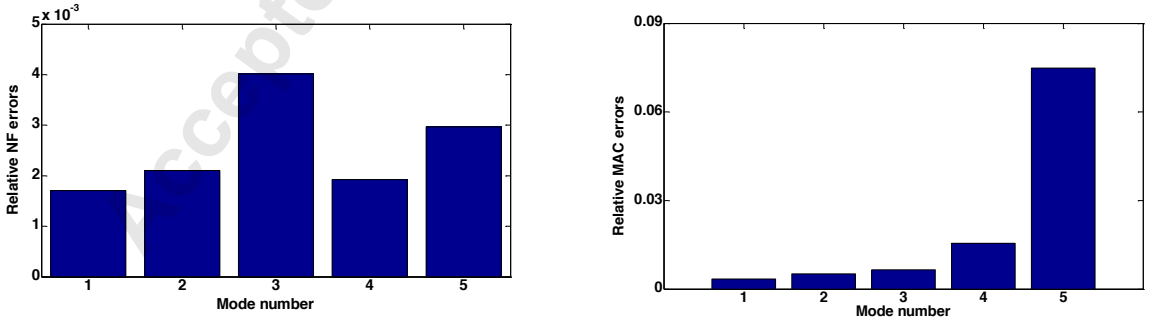

Figure 9 The relative NF and MAC errors of the first five modes

Journal of Vibration and Acoustics. Received October 09, 2015;
Accepted manuscript posted March 6, 2017. doi:10.1115/1.4036110
Rolls-Royce plc

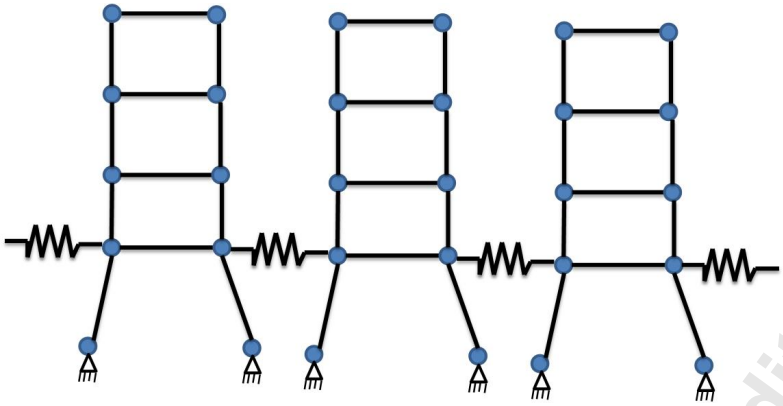

Figure 10 The assembly of the beam frame with coupling springs

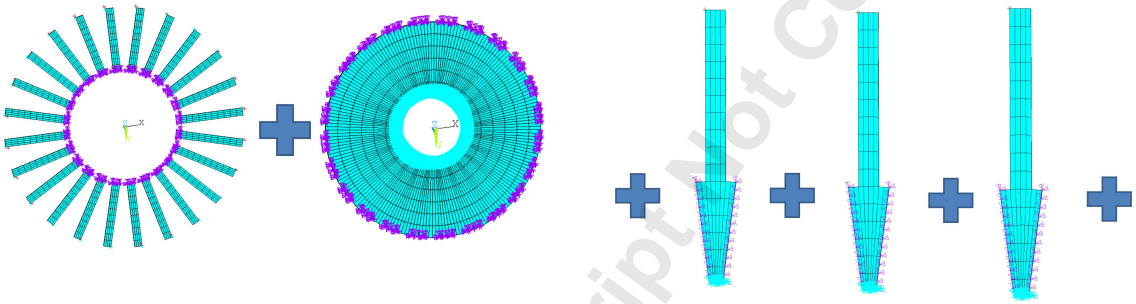

(a) (b)

Figure 11 Two sub-structuring strategies: (a) blade and disc assembly (BDA) (b) bladed disc sector assembly (BSA)

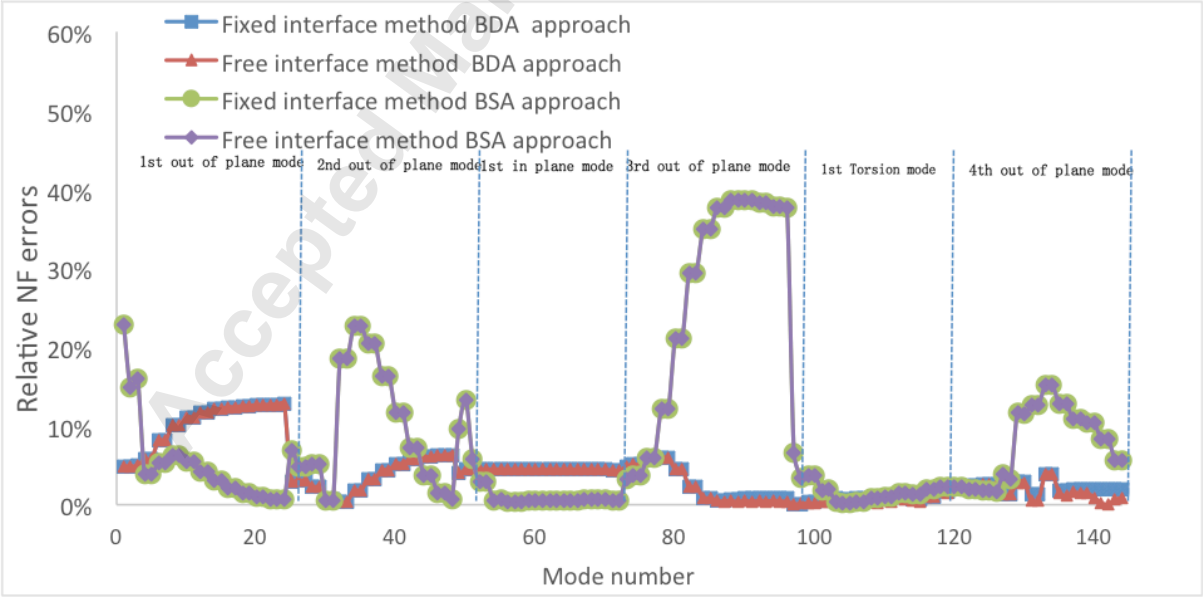

Figure 12 Relative NF errors of the first six flapping mode families provided by the CMS approach with two assembly approaches: (a) BDA and (b) BSA

Journal of Vibration and Acoustics. Received October 09, 2015;
Accepted manuscript posted March 6, 2017. doi:10.1115/1.4036110
Rolls-Royce plc

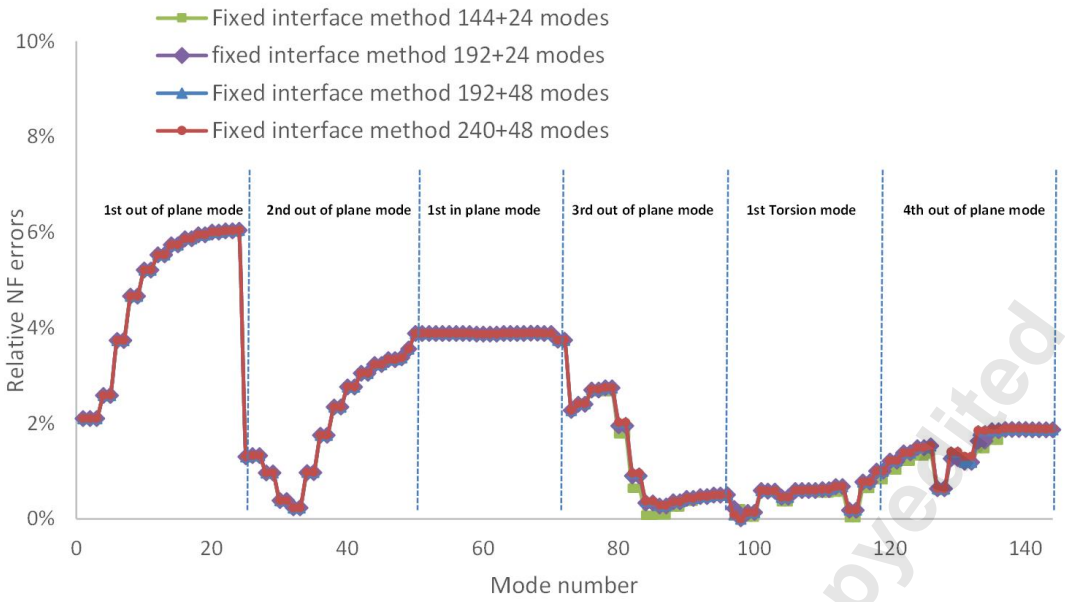

Figure 13 Relative NF errors of the first six flapping mode families using CMS based ROMs with different number of modes as modal bases

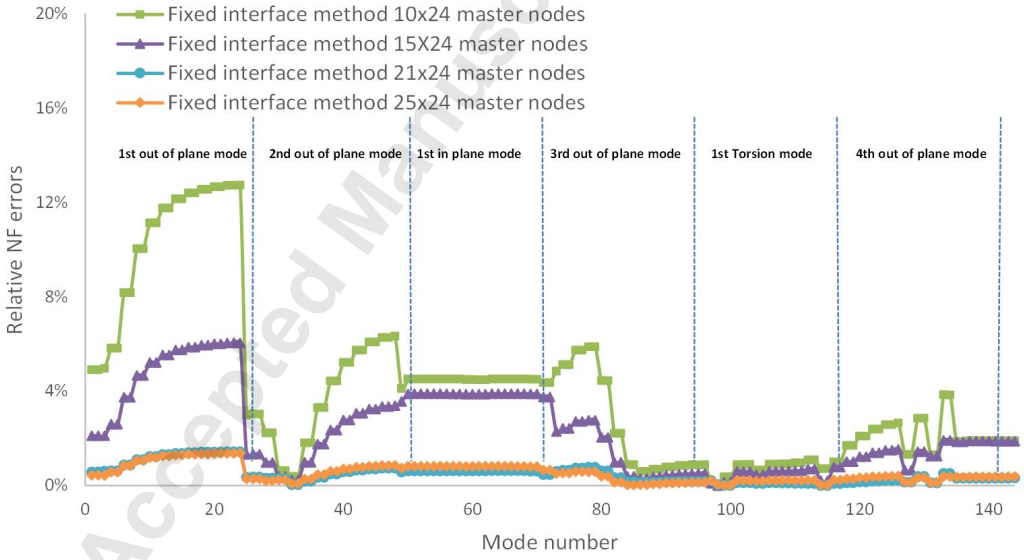

Figure 14 Relative NF errors of the first six flapping mode families using CMS-based ROMs with different number of master nodes as modal bases

Journal of Vibration and Acoustics. Received October 09, 2015;
Accepted manuscript posted March 6, 2017. doi:10.1115/1.4036110
Rolls-Royce plc

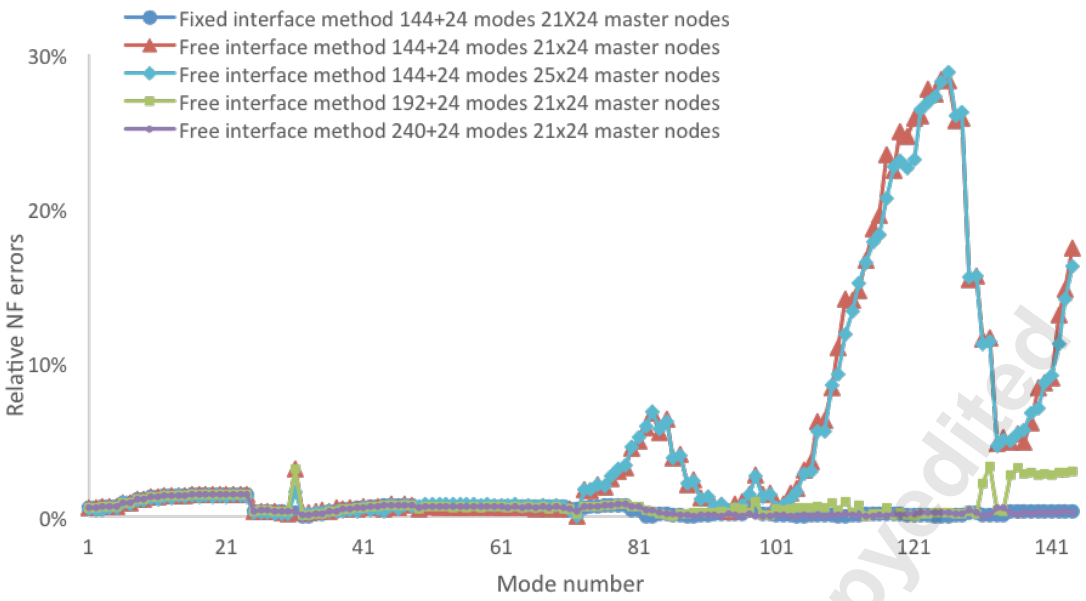

Figure 15 Relative NF errors of the first six flapping mode families using CMS based ROM with two interface methods

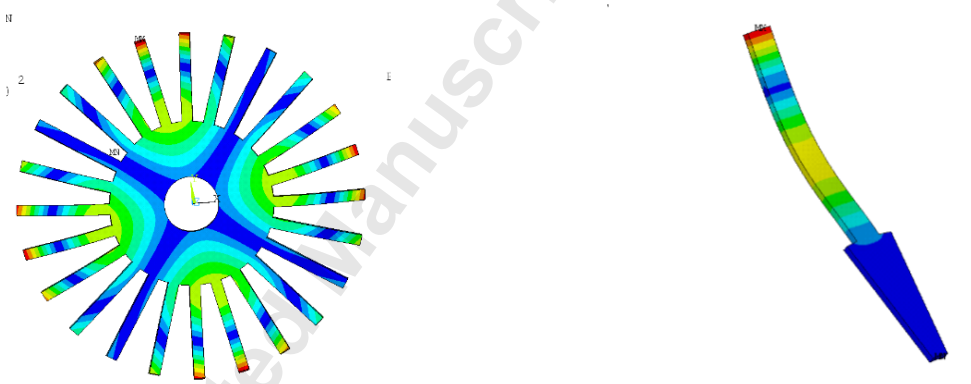

(a) (b)

Figure 16 The modal displacement of (a) the 3rd rotor mode at the 2nd ND (b) the 3rd bladed disc sector mode

Journal of Vibration and Acoustics. Received October 09, 2015;
Accepted manuscript posted March 6, 2017. doi:10.1115/1.4036110
Rolls-Royce plc

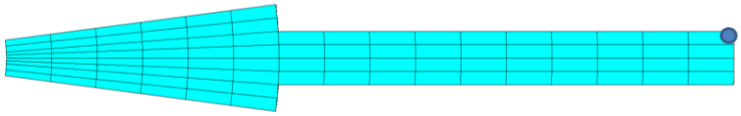

Figure 17 The location of the lumped mass in the representative blade

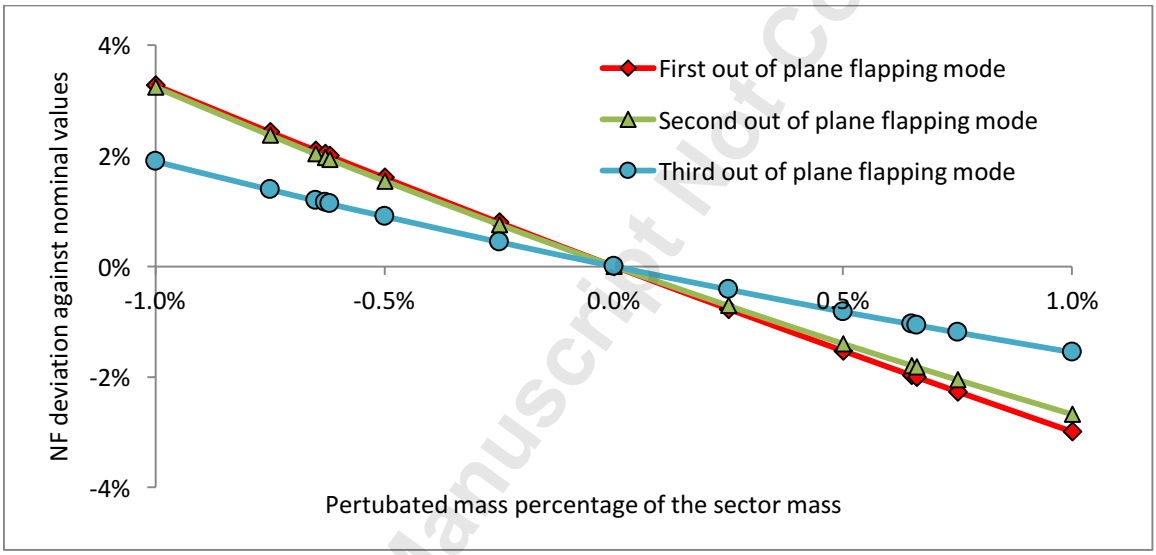

Figure 18 The sensitivity of NFs of the first three out of plane modes to the lumped mass

Journal of Vibration and Acoustics. Received October 09, 2015;
Accepted manuscript posted March 6, 2017. doi:10.1115/1.4036110
Rolls-Royce plc

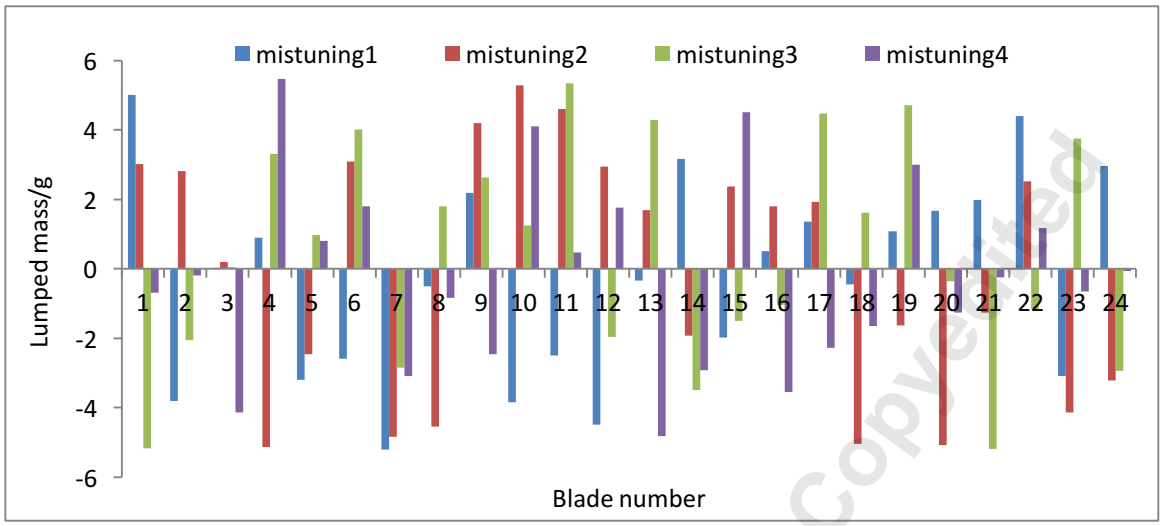

Figure 19 Distribution of lumped masses used in the five mistuning patterns

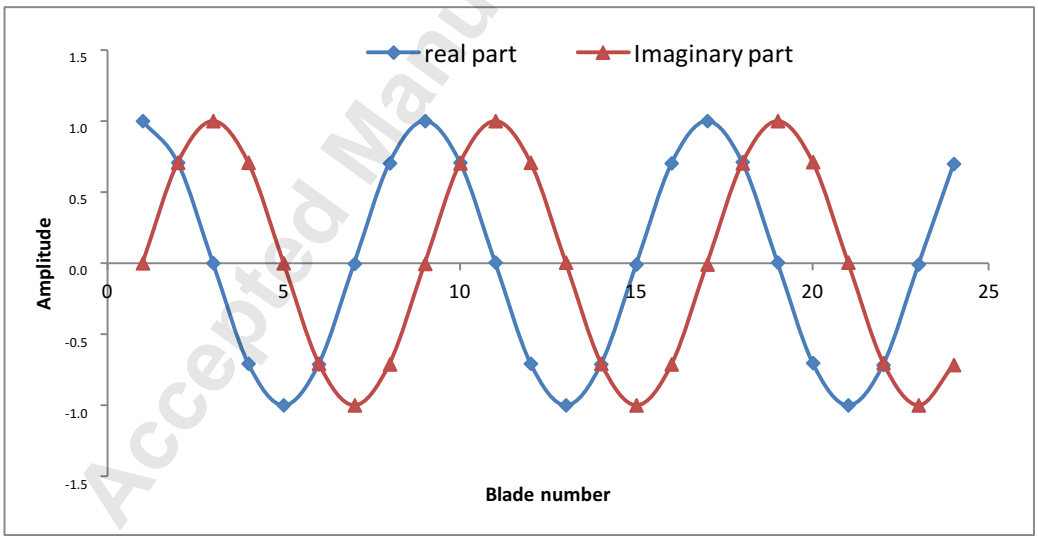

Figure 20 Example of loading distribution for 3nd engine order excitation on the 24 blades

Journal of Vibration and Acoustics. Received October 09, 2015;
Accepted manuscript posted March 6, 2017. doi:10.1115/1.4036110
Rolls-Royce plc

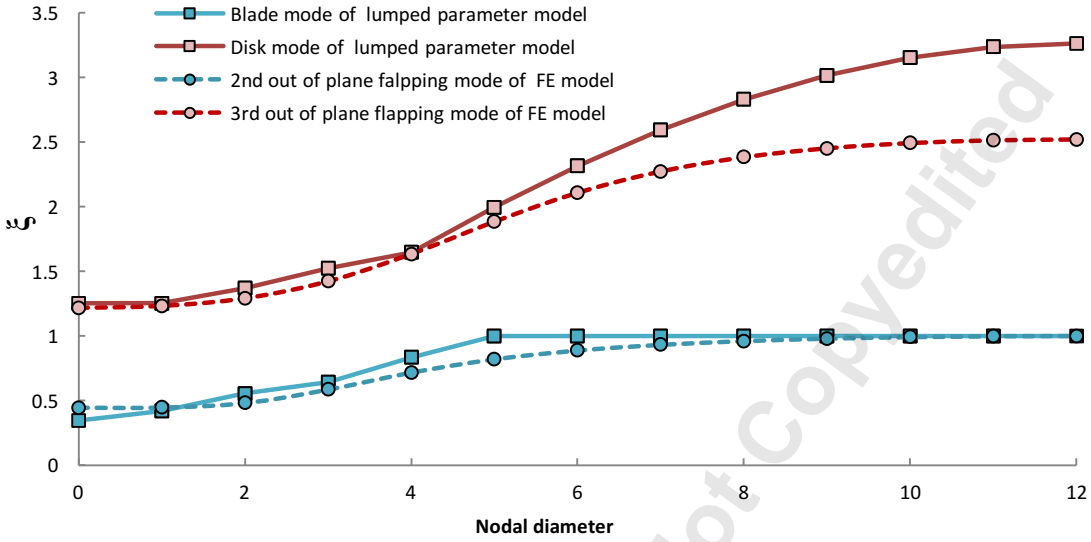

(a)

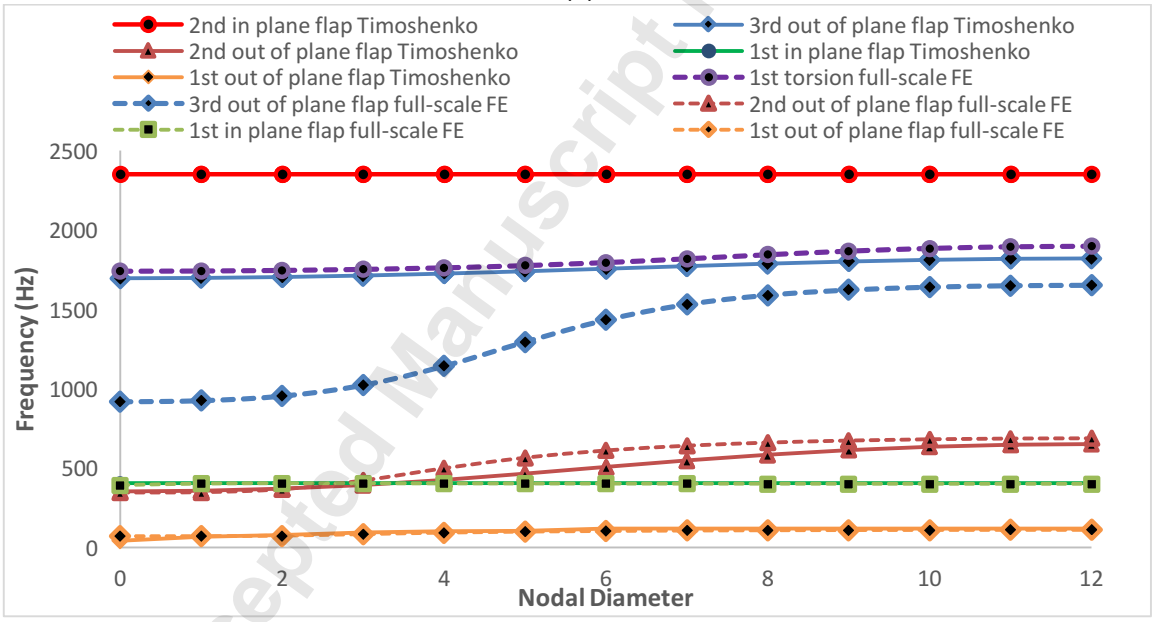

(b)

Journal of Vibration and Acoustics. Received October 09, 2015;
Accepted manuscript posted March 6, 2017. doi:10.1115/1.4036110
Rolls-Royce plc

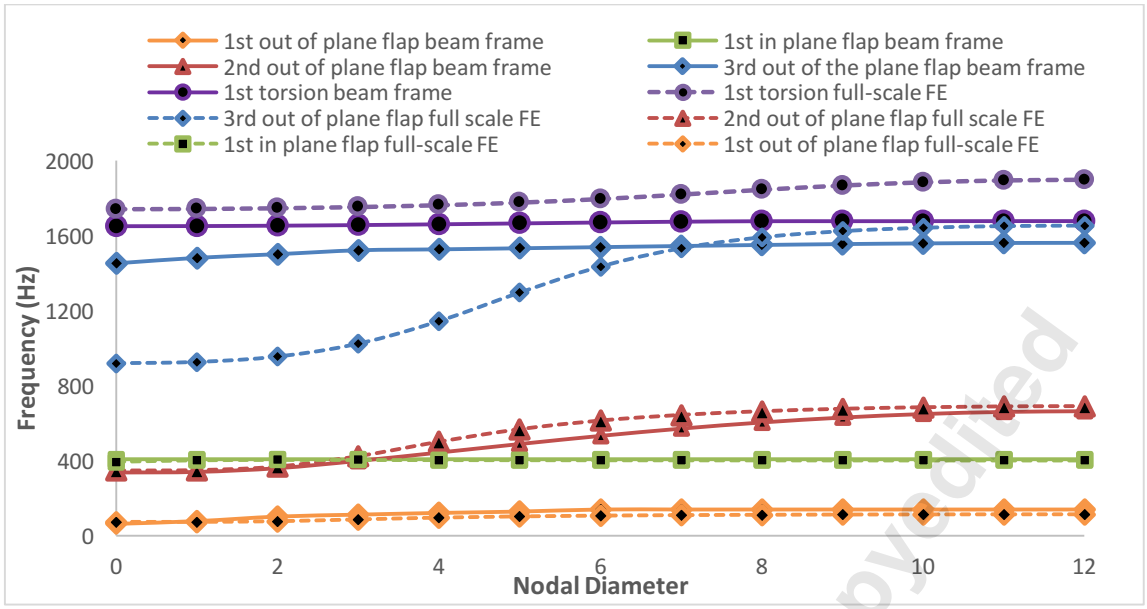

(c)

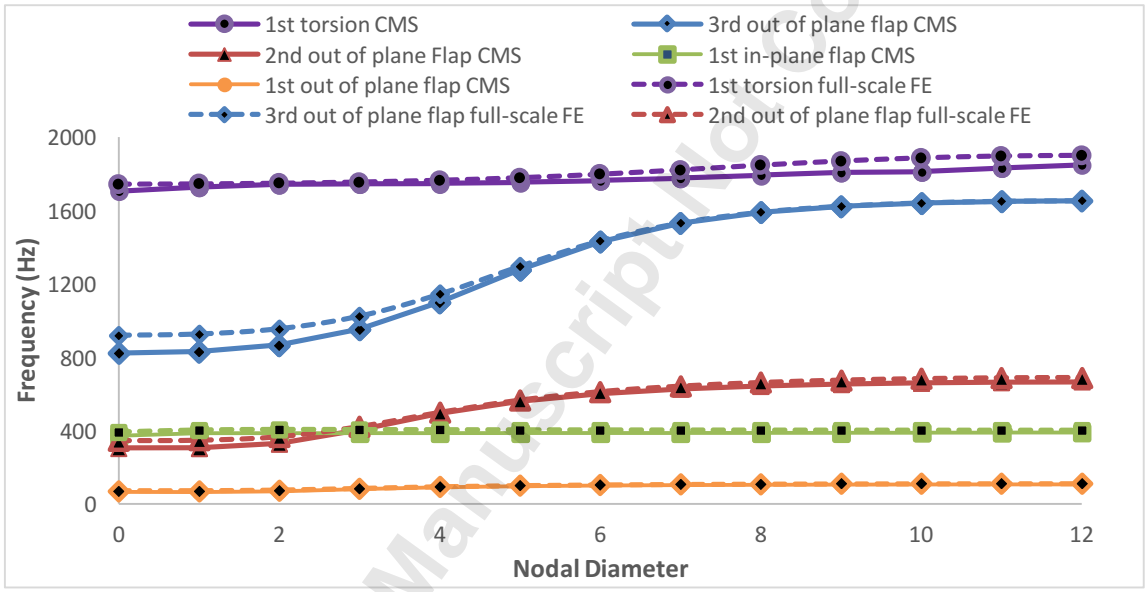

(d)

Figure 21 The variations of the natural frequency with nodal diameter (a) Lumped parameter model (b) Timoshenko beam assembly (c) Beam frame assembly (d) FE-based CMS approach

Journal of Vibration and Acoustics. Received October 09, 2015;
Accepted manuscript posted March 6, 2017. doi:10.1115/1.4036110
Rolls-Royce plc

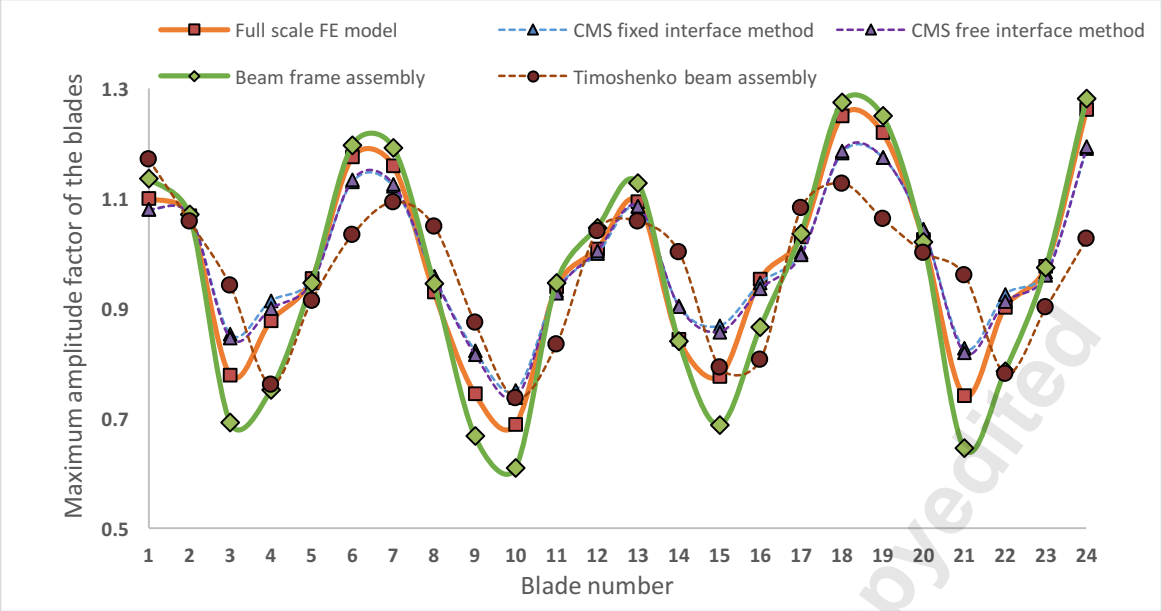

Figure 22 Comparison of the maximum blade amplitude factor between the four ROMs and the full-scale FE model (Fixed interface method:192 modes and 21x24 master nodes; free interface methods:240 modes and 21x24 master nodes)

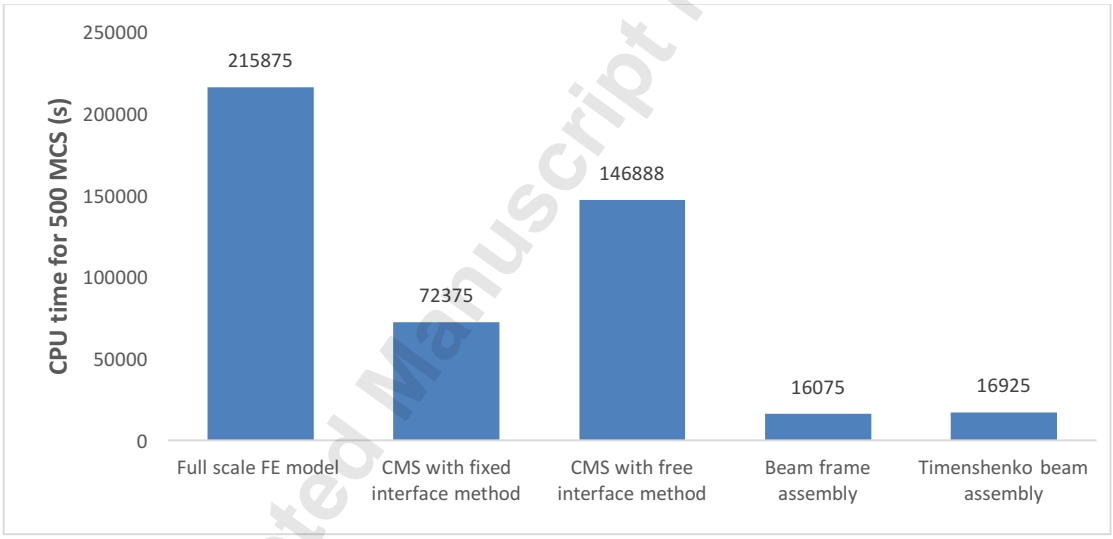

Figure 23 Comparison of the CPU time between three types of ROMs and the full-scale FE model

Journal of Vibration and Acoustics. Received October 09, 2015;
Accepted manuscript posted March 6, 2017. doi:10.1115/1.4036110
Rolls-Royce plc

Table list

Table 1 Parameters identified for lumped parameter model

Parameters	Non-dimensional Values
k^d/k^b	32
k^c/k^b	1500
m^d/m^b	200

Table 2 Comparisons of NFs and mode shapes between the optimized Timoshenko beam and full-scale single blade FE model

Mode number	Timoshenko beam		Errors (Compared to the full-scale FE model)	
	NF (Hz)	Mode shape	NF error	MAC value
1	104	First out of plane bending	6.31%	1.0
2	405	First in plane bending	0.25%	1.0
3	651	Second out of plane bending	15.84%	1.0
4	1822	Third out of plane bending	16.87%	1.0
5	2002	Second in plane bending	17.97%	0.0